Available online at www.sciencedirect.com
ScienceDirect
Bioorganic & Medicinal Chemistry 14 (2006) 8386–8395
Bioorganic & Medicinal Chemistry

Synthesis and evaluation of general mechanism-based inhibitors of sulfatases based on (difluoro)methyl phenyl sulfate and cyclic phenyl sulfamate motifs

Sarah R. Hanson, Lisa J. Whalen and Chi-Huey Wong*

Department of Chemistry and the Skaggs Institute of Chemical Biology, The Scripps Research Institute, 10550 North Torrey Pines Road, La Jolla, CA 92037, USA

Received 24 June 2006; revised 29 August 2006; accepted 6 September 2006
Available online 11 October 2006

Abstract—Several model mechanism-based inhibitors (MbIs) were designed and evaluated for their ability to inhibit sulfatases. The MbI motifs were based on simple aromatic sulfates, which are known to be commonly accepted substrates across this highly conserved enzyme class, so that they might be generally useful for sulfatase labeling studies. (Difluoro)methyl phenol sulfate analogs, constructed to release a reactive quinone methide trap, were not capable of irreversibly inactivating the sulfatase active site. On the other hand, the cyclic sulfamates (CySAs) demonstrated inhibition profiles consistent with an active site-directed mode of action. These molecules represent a novel scaffold for labeling sulfatases and for probing their catalytic mechanism.
© 2006 Elsevier Ltd. All rights reserved.

1. Introduction

By cleaving sulfate esters, sulfatases modulate the activity of a broad range of biological molecules, from small cytosolic steroids to complex cell-surface carbohydrates.[1] These transformations control important cellular events, including lysosomal degradation, hormone regulation, developmental cell signaling, and bacterial pathogenesis.[2–7] Sulfatases are a highly conserved class of enzymes in terms of structure, sequence, and mechanism.[8] They are unique among hydrolytic enzymes in that they have a novel catalytic aldehyde residue, known as α-formyl glycine (FGly), installed post translationally from genetically encoded serine or cysteine precursors.[9,10] For catalysis, FGly is believed to function as an aldehyde hydrate (FGH), wherein a highly nucleophilic geminal hydroxyl performs sulfate transesterification, forming a sulfo-enzyme intermediate (FGS). The second free hydroxyl then collapses the transient FGS, reforming FGly aldehyde and releasing sulfate (Fig. 1).[11] Numerous sulfatases from prokaryotes and eukaryotes bear a generic arylsulfatase (ARS) name, as general activity on small arylsulfate substrates often preceded the discovery of a physiological substrate. Many still have unknown endogenous substrates, especially in bacteria.[1]

Sulfatases have a number of intriguing roles in biological systems. In humans, the importance of sulfatases is underscored by eight clinical disorders, seven of which are lysosomal storage diseases that are known to result from a deficiency in a single sulfatase enzyme.[12] In addition, these enzymes, and potentially all sulfatases, show markedly decreased activity in a rare recessive disorder known as multiple sulfatase deficiency, which has severe and often fatal clinical manifestations.[9] Over the past 10 years, steroid sulfatase, also known as ARSC, has received considerable attention due to its connection to hormone-dependent cancers. ARSC is involved in regulating hormone levels by releasing active steroids and steroid precursors from inactive 4-*O*-sulfate conjugates.

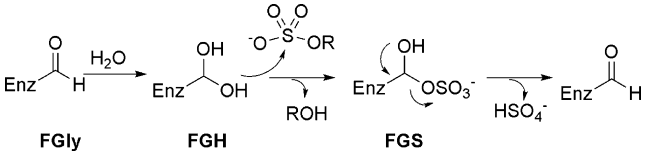

Figure 1. Proposed mechanism for sulfate cleavage by sulfatases involves a unique catalytic aldehyde (FGly).

Keywords: Sulfatase; Inhibition; Mechanism-based inhibition; Proteomics.
* Corresponding author. Tel.: +1 858 784 2487; fax: +1 858 784 2409; e-mail: wong@scripps.edu

0968-0896/$ - see front matter © 2006 Elsevier Ltd. All rights reserved.
doi:10.1016/j.bmc.2006.09.002

When the enzyme is upregulated, higher hormone levels can stimulate hyperproliferative cell activity, which has made ARSC an attractive target for small molecule therapeutics.[13] Recently, sulfatases have been found at the cell-surface, where they dynamically modulate the sulfation states of heparan sulfate proteoglycans (HSPGs). To date, two endo sulfatases that cleave sulfate esters from the 6 position of *N*-acetyl glucosamine sulfate (GlcNAc-6S) in HSPGs have been elucidated.[7,14,15] GlcNAc-6S residues are important for binding signaling molecules such as Fibroblast Growth Factor (FGF), Epidermal Growth Factor (EGF), and wingless (Wnt). When the GlcNAc-6S sulfate group is removed, these molecules can then bind to their cell-surface receptors and initiate signaling cascades. Bacterial sulfatases have also been found to manipulate sulfated oligosaccharides at the cell-surface of mucosal membranes. Such sulfatase activity has been implicated in increased bacterial colonization and severity of infection.[16,17]

Many biological events have been linked to sulfate ester binding, including a host of HSPG-based cell signaling events, inflammation, angiogenesis, cancer metastasis, and viral and bacterial pathogenesis.[1] In an effort to probe sulfatase involvement in these sulfate-dependent events and to further characterize their roles in physiological and pathophysiological processes, we envisaged a proteomic strategy to covalently label the sulfatase enzyme class. Sulfatases are good candidates for a general covalent trap, or mechanism-based inhibitor (MbI), because: (1) they are highly conserved, both structurally and mechanistically, from prokaryotic to eukaryotic members, and (2) most sulfatases exhibit promiscuity with small arylsulfate esters. Therefore, we investigated several MbIs based around the general small arylsulfate substrate that might also be useful for labeling sulfatases (Fig. 3). Herein, we synthesized (difluoromethyl)phenyl sulfates and cyclic 6- and 5-membered phenyl sulfamate structures and evaluated them for MbI activity against an arylsulfatase. Our studies show that cyclic sulfamate scaffolds **5** and **6** inhibit sulfatases in a mechanism-based fashion.

2. Results and discussion

2.1. Strategy and design of mechanism-based inhibitors (MbIs)

In an effort to create useful chemical labeling agents for sulfatases, we investigated MbIs based on general small arylsulfate substrates, as depicted in Figure 2. Two MbI themes were developed based on literature precedent. The first theme, comprised of the (difluoro)methyl phenyl sulfates (DFPSs, **2** and **3**, Fig. 2B), was designed to incorporate a well-known quinone methide trapping scheme (Fig. 3). The second MbI theme, consisting of the cyclic sulfamates (CySAs, **4**, **5**, and **6**, Fig. 2C), was extended from the known irreversible reactivity between linear phenyl sulfamates (such as **1**, Fig. 2A) and steroid sulfatase (ARSC).[18] Model compounds **1**–**6** were synthesized to test for their ability to inhibit sulfatases in a mechanism-based, or specific-irreversible fashion.

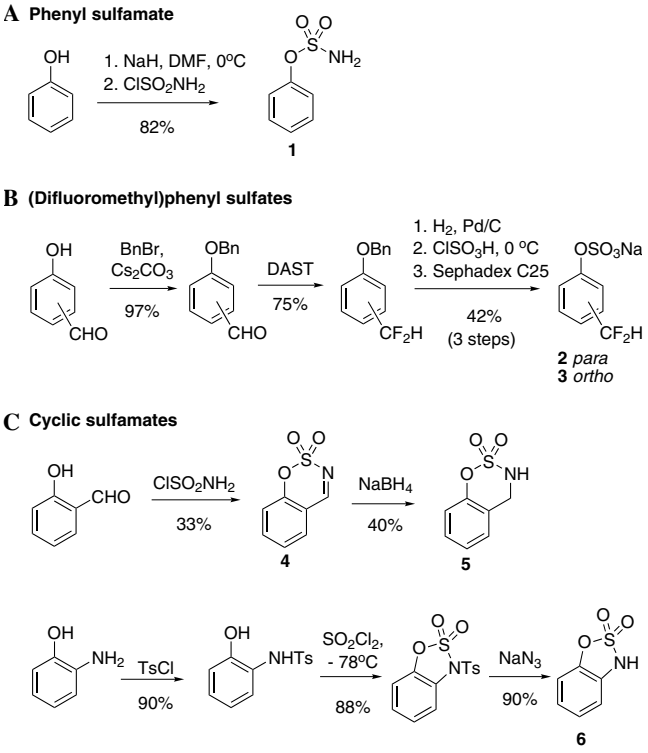

Figure 2. Synthesis of model mechanism-based inhibitors.

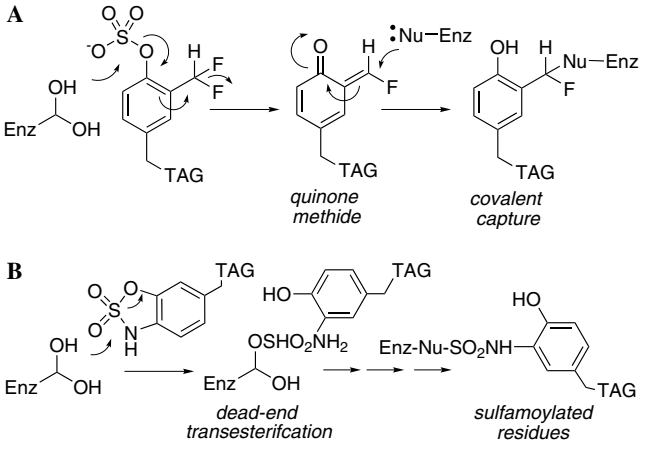

Figure 3. Proposed inactivation by small arylsulfate-based MbIs. Quinone methide trap for sulfatases (A). CySA induced dead-end transesterification or active site nucleophile sulfamoylation (B), see Figure 4 for more detailed evaluation of potential dead-end adducts caused by sulfamates. Both routes offer the advantage of attaching a reporting group (TAG) for further manipulation of inactivated proteins, such as proteomic analysis.

Notably, compounds that inactivate in a mechanism-based manner exhibit several characteristics that can be easily evaluated in the laboratory, including: (1) time- and concentration-dependent inactivation, (2) pseudo-first order loss of activity, (3) saturatable inhibition kinetics, (4) substrate protection, (5) inactivation rates which are unaffected by exogenous nucleophiles, (6) irreversible inactivation, and (7) covalent modification of the enzyme, which can generally be inferred from activ-

ities 1 to 6.[19] We chose an arylsulfatase from *P. aeruginosa* (PARS) as a model sulfatase to test our compounds, since it is highly homologous to human enzymes[20,21] and can be produced and purified in high yield using standard recombinant and affinity purification methods.

2.2. (Difluoro)methyl phenyl sulfates are competitive substrates or inhibitors of PARS

Reactive quinone methide traps have been employed to 'catch' several hydrolytic enzymes.[22] The chemical reaction proceeds as depicted in Figure 3. A quinone methide intermediate is released when the enzyme hydrolytically induces elimination of fluoride from a caged fluoromethyl phenyl substrate. The highly reactive Michael acceptor subsequently captures a properly disposed active site nucleophile, inactivating the enzyme. It seemed likely that the quinone methide trap concept would extend to sulfatases, especially in light of its precedent with phosphatases,[23] which have related structure and mechanism.[24] In fact, this method of sulfatase trapping was also proposed by another laboratory during the course of our studies, although the inhibitory activity was not evaluated.[25] However, kinetic studies for irreversible inhibition of PARS with both *para*- and *ortho*-DFPS (**2** and **3**, respectively) did not show time- and concentration-dependent inhibition. Plots of activity loss against time revealed a straight line, indicating no chemical reaction between inhibitor and enzyme active site (data not shown). Instead, these compounds are likely acting as competitive substrates or inhibitors of the enzyme. When treated as classical competitive inhibitors, the DFPS compounds show K_i values of 29 μM, for the *para* isomer, and 1.3 mM for the *ortho* isomer against PARS (Table 2). The weaker inhibition of the latter is likely due to steric interference at the *ortho* position, as synthesis and evaluation of the isostere 2-methyl-4-nitrophenol sulfate (MNPS) showed a 10-fold increase in K_m versus that of *p*-NPS (Table 1). However, this negative influence at the *ortho* position does not preclude MNPS from being a substrate, which suggests that **2** and **3** might also be processed by the enzyme. The fact that no enzyme labeling occurs suggests that the quinone methide must either rapidly diffuse from the active site or trap a nucleophile, such as water or a non-catalytic amino acid side chain, just outside the pocket. Crystallographic studies of *p*-NPS bound to a human ARS show a disordered phenol ring poking outside of the highly ordered sulfate-bound pocket, suggesting that an active site nucleophile would not be properly poised for attack on the quinone methide.[26] Studies are currently underway to determine if sulfatases may be labeled outside of the active site by the DFPS compounds.

Table 1. Kinetic parameters for PARS substrates

Substrate	K_m (μM)
4MUS	6.6
p-NPS	42
MNPS	550

2.3. Sulfamates and cyclic sulfamates are irreversible inhibitors of PARS

Our next approach toward designing a general sulfatase MbI was garnered by reviewing extensive inhibition studies on human steroid sulfatase (ARSC). Over 10 years ago, arylsulfamates were identified as irreversible inhibitors of ARSC.[27] Indeed, many ARSC-inhibiting scaffolds have been elaborated with sulfamate groups in order to make them more potent irreversible inhibitors.[13] For the most part, sulfamate inhibitors have only been tested against their target ARSC. A few specificity tests, which included human arylsulfatases A and B, showed good to moderate selectivity for ARSC,[13] most likely due to their large hydrophobic cores optimized to interact with the membrane-oriented binding pocket of ARSC.[28] Our experiments showed that the general ARSC pharmacophore (phenyl sulfamate, **1**) also acted as an MbI of PARS. Experiments showed time- and concentration-dependent inhibition of PARS that follow pseudo-first order and saturatable inhibition kinetics, similar to the ARSC enzyme (K_i 4.2 μM, Table 2).[29] This result served nicely to validate our assumption that a general small phenyl sulfate-type MbI would work across the highly conserved sulfatase enzyme class.

Inactivation of sulfatases by phenyl sulfamates could occur by several pathways, as illustrated in Figure 4. Although the precise nature is still unknown, dead-end adducts might result from an irreversible transesterification, sulfamoylation of a catalytic histidine or lysine, formation of a stable sulfonimine species, or an intramolecular Schiff base between the catalytic residues lysine and FGly. Several studies have found an inhibition dependence on the pK_a of various phenyl sulfamates, suggesting that inactivation occurs either concomitantly with, or following, liberation of the associated phenol.[30,31] Additionally, radioactive enzyme was not detected after incubating ARSC with the MbI [^{3}H] estra-

Table 2. Kinetic parameters for PARS inhibitors

Inhibitor	Type	K_i (μM)	k_{inact} (min^{-1})	$t_{1/2}$ (s)	Stability (h)[a]
Phenyl sulfamate (**1**)	Irreversible	4.5	1.23	33.80	24
o-DFPS (**3**)	Competitive	1302	NA	NA	NA
p-DFPS (**2**)	Competitive	29	NA	NA	NA
CySA **4**	Irreversible	NA	NA	NA	<1
CySA **5**	Irreversible	975	0.57	72.95	48+
CySA **6**	Irreversible	401	0.66	63.00	48+

[a] Monitored in sulfatase assay buffer by LCMS.

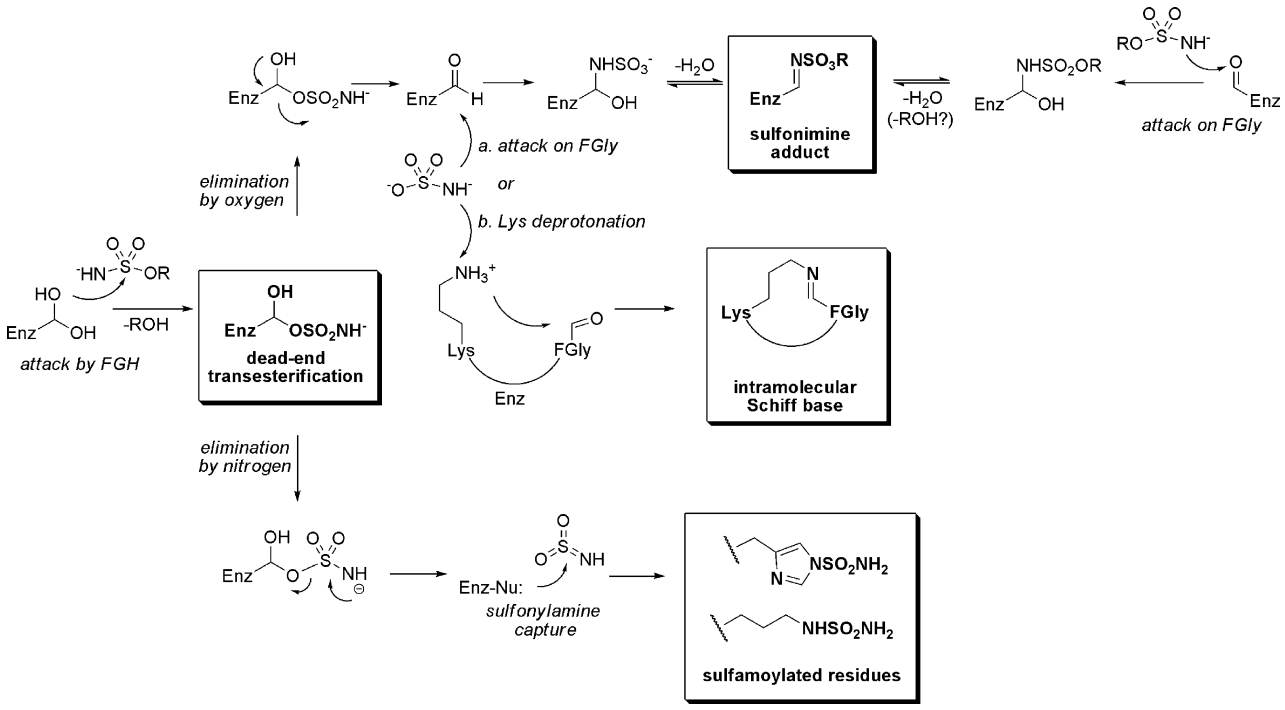

Figure 4. Proposed mechanism-based inactivation pathways for sulfamates. Sulfamates can generate dead-end adducts (boxed intermediates) in the sulfatase active site in a number of ways. The pathway for inactivation is still unknown. Notably, CySAs could also render dead-end adducts resulting from transesterification, sulfamoylation, and formation of an intramolecular Schiff base.

diol-3-*O*-sulfamate, indicating release of sulfamate from its radioactively labeled steroid core.[13] Likewise, in our experiments, when *para* nitrophenol sulfamate was incubated with PARS, a deep yellow solution resulted, indicating liberation of *p*-NP. This situation is not ideal for enzyme labeling, as the covalent modification does not leave any kind of useful chemical handle to attach a reporting group for further analysis of the inactivated protein. However, we imagined that if the sulfamate were cyclized onto the phenyl core, then, in the case of irreversible transesterification, the sulfamate ring might be opened up, while maintaining covalent attachment to both the phenyl ring and the enzyme (Fig. 3B). In the case of sulfonylamine capture, the phenyl ring would also be maintained in the dead-end adduct. Either of these scenarios would provide an opportunity to attach useful reporting groups onto the phenyl ring for further mechanistic and proteomic studies. To explore this modified inhibition route, several simple 5- and 6-membered cyclic sulfamate rings (CySAs **4**–**6**, Fig. 2C) were designed and tested.

Cyclic sulfamates (CySAs **5** and **6**) conformed to well-established criteria for mechanism-based or specific-irreversible inhibition (Figs. 5–9, data shown for **5**). To begin, biochemical profiles reveal that they impart time- and concentration-dependent loss of activity against PARS, which is the hallmark of an irreversible chemical reaction occurring between inhibitor and enzyme active site (Fig. 5). The kinetics of inhibition were biphasic in nature beginning with a fast inactivation phase followed by a slower phase at later time points (biphasic inactivation is visible in Fig. 7). This behavior has been noted in previous studies of sulfamate inhibitors against ARSC and may indicate a combination of inactivation events.[29] However, in the initial few minutes of CySA inactivation, pseudo-first order reaction rates were observed, as seen in Figure 5, from which apparent inactivation rates (k_{obs}) were derived and analyzed by the methods of Kitz and Wilson (see Table 2 for kinetic parameters).[33] Kinetic plots, shown in Figure 6, reveal clear saturation kinetics at higher concentrations of CySA. Such a plateau in inactivation is indicative of an enzyme–inhibitor binding event during the inactivation process, similar to substrate binding in Michaelis–Menten enzyme kinetics. Interestingly, the CySA **4** profile demonstrated varying inactivation slopes for the same inhibitor concentration. In particular, they became more shallow when the inhibitor was dissolved in aqueous buffer for longer periods of time (less inactivation was recorded), suggesting that the compound was unstable. LCMS analysis of **5** and **6** showed compounds to be intact after 48 h in buffer; however, the peaks for **4** were no longer detected after 5 h. Due to instability, CySA **4** was not evaluated further. In the course of our studies, steroidal oxathiazines (modified estrone cores equipped with the CySA **4** functionality) were reported to be stable ARSC inhibitors;[32] however, mechanism-based inhibition was not examined.

Further evidence implicating CySAs **5** and **6** in an active site-directed mode of action was obtained by comparing inactivation rates in the presence of the known substrate, *p*-NPS, and exogenous nucleophiles. Theoretically, the equilibrium achieved between substrate and enzyme and substrate–enzyme complex should protect

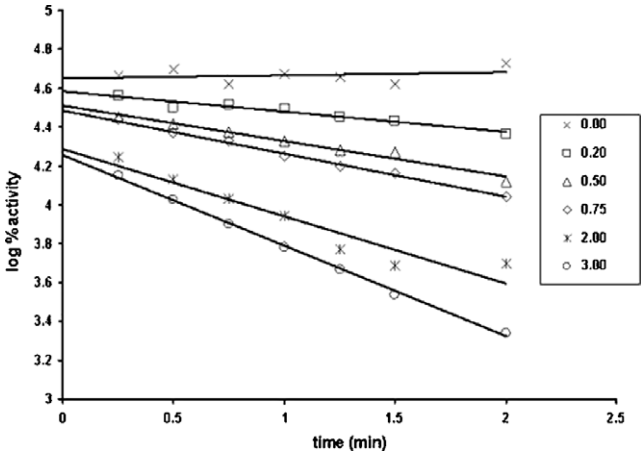

Figure 5. Time and concentration dependent loss of activity. When treated with CySA at various concentrations ([**5**] in mM, left hand box), PARS shows rates (k_{obs}) that are decreasing with time in a pseudo-first order manner. Such behavior indicates an irreversible chemical modification of a catalytic residue.

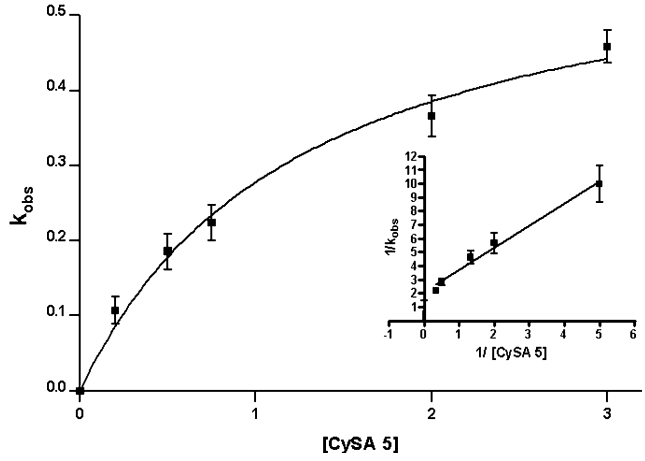

Figure 6. Kinetic inactivation plots by CySA **5**. Saturation kinetics (large plot) indicate that inactivation involves a binding event between enzyme and inhibitor. Non-zero intercepts, as seen on inset double-reciprocal analysis, are also characteristic of a binding step.

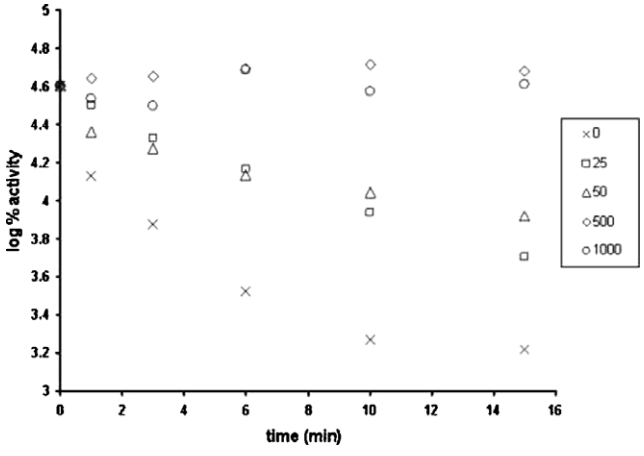

Figure 7. Substrate protection. PARS is protected from CySA **5** inactivation when incubated with increasing concentrations of the substrate *p*-NPS ([*p*-NPS] in μM, left-hand box, 1 mM CySA **5** for all reactions).

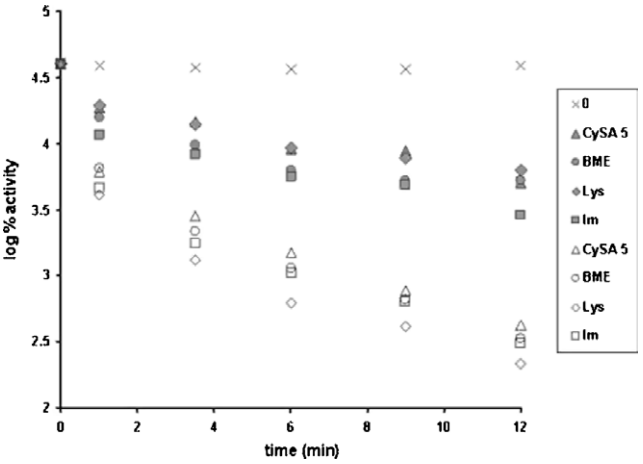

Figure 8. Effect of exogenous nucleophiles. Common biological nucleophiles (β-mercaptoethanol (BME, circles), lysine (Lys, diamonds), and imidazole (Im, squares), and were added to a final concentration of 1 mM in the presence of CySA *5* (without nucleophiles, triangles) at 0.5 and 1 mM (filled and open data points, respectively). Data is consistent with an inactivating species that is triggered and captured within the active site, as rates are unaffected.

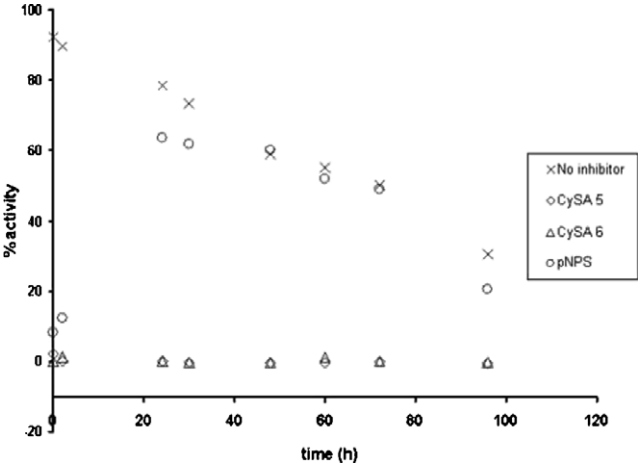

Figure 9. Recovery of activity. PARS was treated with *p*-NPS or CySAs before dialysis over an extended period of time. After incubation with *p*-NPS (circles), sulfatase activity returned to normal values (untreated activity shown by cross marks). However, samples exposed to CySA (**5** diamonds and **6** triangles) are permanently inactivated. Remaining activity is expressed as a percentage of a standard (untreated and undialyzed PARS).

from the formation of enzyme–inhibitor complex that ultimately leads to inactivation. As depicted in Figure 7, when substrate was dosed into the incubation mixture at 25 μM, a significant amount of PARS activity remained when compared to the control levels, without any *p*-NPS. In fact, at a concentration above 500 μM *p*-NPS, which is twice the concentration of **5**, no significant loss of PARS activity was observed over the measured time course. Likewise, since mechanism-based inhibition leading to enzyme-adduct should be solely a function of binding, catalysis, and then inactivation, all within the active site, exogenous nucleophiles should not affect the inactivation rates. In a case where electrophilic reactive species were diffusing from the active site

before re-entering to cause inactivation, exogenous nucleophiles would be expected to quench these intermediates, resulting in much slower inactivation rates. In addition, if the molecules were unstable to exogenous nucleophiles, or were susceptible to activation by them, dramatic changes in inactivation rates would also be expected (as seen previously with CySA **4**). To address this issue, representative amino acid nucleophiles, including β-mercaptoethanol (cysteine-type), imidazole (histidine-type), and lysine, were added to a standard time- and concentration-dependent inactivation assay using CySA inhibitors. As shown in Figure 8, addition of biological nucleophiles at 1 mM to incubation mixtures containing either 1 or 0.5 mM of **5** or **6** did not show any appreciable difference in inactivation rates. Together, these results strongly support that sulfatase inactivation by CySA requires initial catalytic turnover in the active site.

Tight binding inhibitors, which are often included in the realm of mechanism-based inhibitors, also display time- and concentration-dependent inhibition, substrate protection, and unaffected inhibition rates in the presence of nucleophiles; however, they do not chemically modify the enzyme. To distinguish between an irreversible and a tight-binding inhibitor, extended dialysis is often used. In the case of the tight-binding inhibitor, dialysis over long periods of time in the presence of large volumes of buffer should cause the molecule to dissociate, resulting in the return of enzyme activity; whereas a covalently labeled enzyme will never regain activity. As shown in Figure 9, after an overnight incubation with CySAs **5** and **6**, PARS remained inactive, even after 4 days of dialysis. In comparison, PARS incubated with high concentrations of the substrate *p*-NPS steadily regained activity, quickly achieving untreated enzyme activity. These data further substantiate that PARS is irreversibly inactivated by CySAs **5** and **6**.

Interestingly, previous structure–activity relationships with ARSC showed that N-alkylation of phenyl sulfamates resulted in much weaker, competitive inhibitors.[34] However, herein, it is demonstrated that by cyclizing the sulfamate to the phenyl core, irreversible inhibition can be maintained. Possibly, abrogation of activity by N-alkylation is a steric effect. Crystallographic studies show that the sulfate binding pocket is a narrow, highly polar environment that is unlikely to tolerate much more bulk than afforded by the sulfate group.[11,21,28,35] Apparently, the more rigidly confined cyclic sulfamates are capable of presenting their reactive moiety into the sulfatase active site, although higher K_i values when compared with the smaller phenyl sulfamate **1** indicate a less ideal binding situation (Table 2). Given that inactivation still occurs when using CySA inhibitors, it seems unlikely that a sulfonimine moiety is the dead-end adduct generally caused by sulfamate inactivation (Fig. 4). However, the inactivation rates, which are likely a combination of several rate constants leading to active site modification, of CySAs **5** and **6** differ slightly from **1**, indicating that their rate-limiting steps may be different, or they might have a different inhibition route altogether. One possibility for sulfamate inactivation that has not been proposed previously is that the sulfamate nitrogen deprotonates one of the two active site lysines that are in close proximity to FGly, prompting the formation of an irreversible internal Schiff base. Research into the precise nature of the dead-end adducts cased by the CySAs is ongoing.

3. Conclusion

Sulfatases are an interesting class of enzymes with emerging biological relevance in the fields of cancer, developmental cell signaling, and pathogenesis. Their involvement in cleaving sulfate esters in the heparan sulfate proteoglycans makes them particularly attractive as chemoenzymatic tools to manipulate and study the myriad of intricate sulfate-dependent binding events that occur at the cell-surface. Our interest in discovering and monitoring the activity of sulfatases led to the investigation of potential mechanism-based inhibitors (MbIs) that could also function as useful reactive labels (Fig. 3). We modeled our MbIs around small arylsulfates, which are broadly accepted as substrates across the sulfatase enzyme class. In support, we tested a known MbI of human steroid sulfatase, the phenyl sulfamate motif, and showed that it is also active against an arylsulfatase from bacteria (PARS) when displayed on a simple phenyl ring (**1**). Furthermore, by cyclizing the sulfamate motif to 5- and 6-membered rings (CySA **6** and **5**, respectively), novel specific-irreversible inhibition was observed. This behavior lends some new insight into the mechanism of dead-end inactivation of sulfatases by phenyl sulfamates (Fig. 4). For example, the sulfonimine adduct is unlikely to be an irreversible covalent adduct since the CySA structures preclude such formation. Also, barring that sulfamates trigger the formation of an internal Schiff base, it seems likely that the CySAs might covalently label the enzyme while leaving the phenol ring still attached (Fig. 3). Currently, studies are underway to determine precisely how CySAs shut down sulfatase activity. Also, we are working toward appending the phenol with different reporter groups, including biotin and fluorescent molecules, so that the labeled enzymes can be selected for further studies, such as activity-based proteomic profiling.[36]

4. Experimental

4.1. Chemistry

Commercially available reagents were purchased from Sigma-Aldrich and used as supplied unless stated otherwise. Solvents were purified and dried by standard procedures and distilled prior to use. Flash chromatography was performed with Silia P Flash Silica Gel (40–63 μM, 60 Å, Silicycle). Thin-layer chromatography was performed with EMD silica gel 60 F_{254}, regular phase precoated plates. Proton NMR spectra (^{1}H NMR) were recorded at 500 MHz or 400 MHz. Chemical shifts are expressed in parts per million (δ) and are referenced to residual protium in the NMR solvent: CD_2HOD, δ 3.31; $CHCl_3$, δ 7.26. Carbon NMR (^{13}C NMR) spectra

were recorded at 100 MHz. Chemical shifts (δ ppm) are referenced to the carbon signal for the solvent: CD_3OD, 49.15; $CDCl_3$, 77.23. Liquid chromatography mass spectral (LCMS) analysis was performed using an Agilent 1100 LC coupled to an Agilent 1100 single quad mass spectrometer with 4.6 mm × 50 mm C8 column and the mobile phases of 100% H_2O/0.1% formic acid and 100% ACN/0.1% formic acid.

4.1.1. Synthesis of 2-methyl 4-nitrophenyl sulfate (MNPS). Sulfonation of 2-methyl 4-nitrophenol was carried out according to a previously developed protocol.[37] Briefly, in a flamed-dry flask under Ar, 2-methyl 4-nitrophenol (286 mg, 1.86 mmol) was dissolved in a solution of carbon disulfide (2 mL) and *N*,*N*-dimethylaniline (DMA, 1.2 mL, 7.44 mmol) at 0 °C. The dropwise addition of chlorosulfonic acid (ClSA, 86 μL, 2.79 mmol) resulted in the evolution of gas and formation of two phases and then the reaction mixture was allowed to warm to ambient temperature. After 18 h, ice-cold aq KOH (536 mg, 13.4 mmol, in 5 mL water) was added. The aqueous phase was extracted once with warmed toluene (25 mL), twice with ether (50 mL), and then concentrated in vacuo to obtain an orange solid. The product was recrystallized in basic water (pH 10) to obtain yellow crystals of the MNPS potassium salt (120 mg, 0.44 mmol, 24% yield for first recrystalization). ^{1}H NMR (D_2O, 400 MHz): 3.49 (s, 3H), 6.21 (d, 1H); 6.77 (dd, 1H); 6.86 (d, 1H). MS-ESI 231.9 $[M-H]^-$.

4.1.2. Preparation of sulfamoyl chloride. A fresh solution was prepared for each reaction, based on a modified procedure.[31] Chlorosulfonyl isocyanate (1.2 mL, 14.1 mmol, 5 equiv) was dissolved in CH_2Cl_2 (7 mL) under Ar at rt, then cooled to 0 °C. In a separate flask, formic acid (99%, 0.54 mL, 5 equiv) was dissolved in CH_2Cl_2 (3 mL) at rt. The formic acid solution was then added dropwise to the isocyanate slowly over 10 min. Slow, steady evolution of CO_2 was observed; eventually a fine white precipitate formed. After 10 min, the ice bath was removed and the reaction mixture was warmed to rt, then stirred for 1 h, before use in the next reaction.

4.1.3. Synthesis of phenyl sulfamates (1). Using a standard procedure for sulfamoylation,[31] phenol (1.2 mmol, 1.0 equiv) was dissolved in DMF and cooled to 0 °C under anhydrous conditions. To the phenolic solution, sodium hydride (3.6 mmol, 3.0 equiv) was added over 10 min and allowed to stir for 1 h. A solution of freshly prepared sulfamoyl chloride (6.2 mmol, 5 equiv, Section 4.1.2) was subsequently added over 5 min and the reaction mixture was warmed to ambient temperature. After 2 h, the reaction was quenched with methanol and partitioned between EtOAc and brine. The organic layer was dried over $MgSO_4$ and purified on silica using a 1:30 EtOAc/CH_2Cl_2 solvent system to produce the white solid **1** (0.98 mmol in 82% yield). ^{1}H NMR ($CDCl_3$, 400 MHz): 7.31–7.33 (m, 3 H); 7.39–7.43 (m, 2H). ^{13}C NMR ($CDCl_3$, 100 MHz): δ 124.94, 130.24, 132.79. MS-ESI 172.0 $[M-H]^-$.

4.1.4. Synthesis of (difluoro)methyl phenyl sulfates (DFPS, para-2 and ortho-3). To a room temperature solution of salicylaldehyde (1 mL, 9.4 mmol) and cesium carbonate (3.36 g, 10.3 mmol) in DMF (5 mL) was added benzyl bromide (1.23 mL, 10.3 mmol), under anhydrous conditions. After 6 h, the reaction mixture was extracted with EtOAc and water. The organic layer was concentrated and flashed over silica (1:20 EtOAc/hexanes) to produce a clear oil (1.88 g, 8.9 mmol, 97% yield). The benzylated product (1.6 g, 7.5 mmol) was subsequently dissolved in dry CH_2Cl_2 (4 mL) and treated with DAST (1.68 mL, 12.8 mmol), a drop of dry MeOH was introduced to catalyze the reaction. The reaction was quenched with satd aq $NaHCO_3$ after 5 h, extracted three times with CH_2Cl_2 (100 mL), and then purified by flash chromatography (3:100 EtOAc/hexanes) to yield a clear oil (1.3 g, 5.6 mmol, 75% yield). The resulting (difluoro)methyl benzyl phenol (640 mg, 2.7 mmol) was submitted to hydrogenolysis under acidic conditions using Pearlman's catalyst ($Pd(OH)_2$, cat.) in MeOH (12 mL) with AcOH (0.6 mL) under an atmosphere of hydrogen. The unstable phenol was quickly passed through Celite, concentrated, and sulfonated using chlorosulfonic acid, (273 μL, 4.1 mmol) and DMA (1.56 mL, 12.3 mmol) as described in Section 4.1.1. The DFPS product was purified by flash chromatography (1:4 MeOH/CH_2Cl_2 with 0.1% TEA) and then passed through an ion exchange resin (Sephadex C25, washed with 1 M NaOH and equilibrated in H_2O) to obtain the sodium salt (483 mg, 42% over 2 steps). Compound **2** (*para isomer*): ^{1}H NMR (D_2O, 400 MHz): δ 6.81 (t, J = 56.0 Hz, 1H); 7.40 (d, J = 8.4 Hz, 2H); 7.61 (d, J = 8.4 Hz, 2H). ^{13}C NMR (D_2O, 100 MHz): δ 119.9, 125.0, 125.5, 125.6 (t, J = 170 Hz), 160.4. ^{19}F NMR (D_2O, 400 MHz) 109.1 (2F). MS-ESI 223.0 $[M-H]^-$. Compound **3** (*ortho isomer*): ^{1}H NMR (MeOD, 400 MHz): δ 7.09 (t, J = 37 Hz, 1H); 7.26 (m, 1H); 7.43–7.57 (m, 3H). ^{13}C NMR (MeOD, 100 MHz): δ 113.0 (t, J = 159 Hz) 123.6, 126.3, 126.8 (t, J = 2.8 Hz), 132.7, 164.6. ^{19}F NMR (MeOD, 400 MHz) 112.7 (2F). MS-ESI 223.0 $[M-H]^-$.

4.1.5. Synthesis of 6-membered unsaturated cyclic sulfamate (4). Salicylaldehyde (0.3 mL, 2.8 mmol) was dissolved in CH_2Cl_2 (14 mL) under Ar at rt. Triethylamine (1.8 mL, 14.1 mmol) was added to the reaction mixture which was then cooled to 0 °C. The freshly prepared sulfamoyl chloride (14.1 mmol, Section 4.1.2) was then added to the salicylaldehyde dropwise by cannula over 15 min. After stirring overnight, the reaction mixture was dark red. It was re-cooled to 0 °C then quenched with satd aq NH_4Cl. The reaction mixture was then washed once with water and the layers were separated. The aqueous phase was washed once with CH_2Cl_2, then the combined organic layers were washed once with satd aq NaCl, dried over Na_2SO_4, and concentrated to give a red syrup. The syrup was adsorbed on silica gel, using CH_2Cl_2 as solvent, then purified by flash chromatography over 100 mL silica, eluting with 9:1 hexanes/EtOAc, 8:2 hexanes/EtOAc, and 6:4 hexanes/EtOAc, yielding 0.17 g (33%) of a pinkish solid. Upon exposure to air for 1 h, solutions containing the product turned a faint pink color. ^{1}H NMR ($CDCl_3$, 400 MHz): δ 8.69 (s, 1 H); 7.79–7.75 (m, 1H); 7.72 (dd, J = 1.6, 7.7 Hz, 1H); 7.46 (dt, J = 0.9, 7.6 Hz, 1H); 7.28 (d, J = 8.2 Hz,

1H). ^{13}C NMR ($CDCl_3$, 100 MHz): δ 167.9, 154.0, 137.7, 130.9, 126.2, 118.5, 115.2.

4.1.6. Synthesis of 6-membered cyclic sulfamate (5). Compound **4** (0.17 g, 0.9 mmol, 1 equiv) was dissolved in CH_3OH (5 mL) under Ar then cooled to 0 °C. $NaBH_4$ (38 mg, 1.0 mmol, 1.1 equiv) was added to the reaction. After 30 min, TLC (1:1 hexanes/EtOAc) showed completion of the reaction. Silica gel was added and the reaction mixture was concentrated to dryness, then flashed over 100 mL silica, eluting with 8:2 hexanes/EtOAc then 7:3 hexanes/EtOAc. This provided 0.073 g (43%) of a white solid. ^{1}H NMR ($CDCl_3$, 400 MHz): δ 7.34–7.30 (m, 1H); 7.25–7.16 (m, 2H); 6.98 (dd, J = 8.3, 0.99 Hz, 1H); 4.58 (s, 2H). ^{13}C NMR ($CDCl_3$, 100 MHz): 154.0, 129.9, 127.9, 125.9, 120.5, 119.2, 46.9. MS-ESI 184.0 $[M-H]^-$.

4.1.7. Synthesis of 5-membered cyclic sulfamate (6). Prepared according to Method B in Andersen et al.[38] with the exception that sodium azide was used for removal of the tosylate group.[39]

4.2. Biology

Commercially available reagents were purchased from Sigma-Aldrich and used as supplied unless stated otherwise. The PARS gene was kindly provided by Professor Michael Kertesz on the plasmid pME4322. All assays were performed in triplicate in Costar 96-well microtiter plates, black for fluorescent assays or clear for colorimetric assays. Responses were monitored using a Fusion spectrophotometer (Perkin-Elmer).

4.2.1. *Pseudomonas aeruginosa* arylsulfatase: subcloning, expression, and purification. Arylsulfatase (ARS) from *P. aeruginosa* (PARS) was chosen because it is a tractable and well-characterized sulfatase, showing high homology with human enzymes.[20,21] The gene (*astA*) was amplified via standard polymerase chain reaction (PCR) using Vent polymerase from vector pME4322.[20] The forward gene primer (5′-CAATTCCCTCTA GAAATTTG-3′) was engineered to contain the *Xba*I restriction site, while the reverse gene primer (5′-GGTGGTGGTGCTCGAGTCGTCGCSCCAGGAA AGGCG-3′) contained a *Xho*I restriction site and C-terminal hexahistidine tag. The amplified fragment was doubly digested (*Xho*I, *Xba*I; New England Biolabs) and ligated (T4 DNA ligase, Roche) into pET28a (Invitrogen) linearized under identical restriction conditions. The new subclone, pSH1.2, was sequenced for accuracy and transformed into DH10B for storage. To obtain PARS protein, pSH1.2 was transformed into BL21(DE3) *Escherichia coli* (Invitrogen) cells and grown to OD600 of 0.8 in Luria–Bertani (LB) broth under constant agitation (250 rpm) and temperature (37 °C). IPTG was then added to a final concentration of 1 mM and the cells were allowed to expand for 6 h at 37 °C. Cells were spun down (3000 rpm, 20 min), washed with phosphate-buffered saline (from PBS tablets), re-pelleted, and frozen at −20 °C. The cell pellet was reconstituted in cell lysis buffer (50 mM phosphate, 150 mM NaCl, and 10 mM imidazole, pH 8.0) and passed three times through a French press (15,000 psi). Cellular debris was cleared by centrifugation (10,000 rpm, 20 min) and the soluble lysate was passed through a nickel–NTA affinity purification column under gravity. Native purification proceeded as described (Qiagen, Native purification protocol). Protein was dialyzed (mini dialysis units, MWC 10 kDa, Pierce), concentrated to 3 mg/mL in 100 mM Tris, pH 7.5, with 20% v/v glycerol, and stored at −20 °C. Protein dilutions at 0.1 mg/mL were stable for at least a month at 4 °C.

4.2.2. Catalytic assay. Sulfatase activity was determined by incubating PARS (1 μg/mL) in sulfatase assay buffer (100 μM 4-methylumbelliferone sulfate (4MUS), 100 mM Tris, pH 8.9) at 30 °C. Formation of 4-methylumbelliferone was monitored spectrophotometrically (λ_{ex} 360, λ_{em} 450) over 2 min. In addition two other colorimetric substrates of PARS were evaluated including commercially available *p*-nitrophenol sulfate (*p*-NPS) and synthetic 2-methyl 4-nitrophenol sulfate (MNPS). In both cases, the release of a nitrophenol (NP) species was monitored at 402 nm. Common kinetic parameters such as K_m and K_i for competitive inhibition were determined using standard non-linear fitting techniques according to standard Michaelis–Menten enzyme kinetic equations (Prism Graph). All assays were performed in triplicate for accuracy.

4.2.3. Time- and concentration-dependent inactivation assay. PARS was incubated with various inhibitor concentrations from 0.25 to 2 min time intervals, before being diluted into sulfatase assay buffer to measure catalytic activity. The values for remaining activity (A) for a given inhibitor concentration at a given time were converted into natural log percentage values of the original enzyme activity (A_0) and were plotted against total incubation time (t) to determine the nature of inhibition. As determined by Kitz and Wilson, in the case of specific, or active site-directed, irreversible inhibition, a saturatable pseudo-first order rate constant (k_{obs}) for inactivation is observed over time, as described by Eqs. 1 and 2.[33]

$$\ln A/A_0 = -k_{incat} * t/(1 + K_i/I) \quad (1)$$

$$k_{obs} = -k_{inact}/(1 + K_i/I) \quad (2)$$

$$1/k_{obs} = 1/k_{inact} - K_i/(K_{inact} * I) \quad (3)$$

when the double-reciprocal of Eq. 1 is replotted, as described in Eq. 3, saturatable inactivation is revealed by non-zero intercepts at y ($1/k_{inact}$, where k_{inact} is the apparent zero order rate constant for enzyme inactivation) and x ($1/K_i$, where K_i is the Michaelis constant for inhibitor). Notably, the double-reciprocal plot of a non-specific irreversible inhibitor, such as a general acylating agent, would proceed through the origin.[33]

4.2.4. Substrate protection and exogenous nucleophiles. Time- and concentration-dependent inactivation of PARS was evaluated in the presence of a known sulfatase substrate and representative amino acid nucleophiles. Activity was monitored as described previously (see Section 4.2.3), except that either a general sulfatase

substrate, *p*-NPS, or an exogenous nucleophile was added to the incubation mixture. In order to determine if a sulfatase substrate provided protection against inhibitor inactivation, the concentration of *p*-NPS was varied from 0.025 to 1 mM in the presence of inhibitor. For studying the effects that exogenous nucleophiles have on inactivation rates, β-mercaptoethanol (cysteine-type behavior), imidazole (histidine-like behavior), and lysine were added to a final concentration of 1 mM in the presence of inhibitor. In all cases, inactivation rates were compared with those of PARS and inhibitor-only controls.

4.2.5. Recovery of activity following inactivation. PARS (10 μg/mL) was mixed with 5 mM inhibitor. Additionally, control samples of PARS incubated alone, as well as, in the presence of 5 mM *p*-NPS were performed. After an overnight incubation, the samples were subjected to extensive dialysis in microdialysis units (Pierce). Dialysis buffer (1 L, 100 mM Tris buffer, pH 8.9) was changed every 3 h for the first 12 h and then every 12 h for the remainder of the experiment. At various time points, 5 μL aliquots of dialysate were removed and diluted 1/20 in sulfatase assay buffer to determine catalytic activity. Activities were normalized to percentage activity of untreated and undialyzed protein standard.

Acknowledgments

This work was supported by the NIH and the Skaggs Institute for Chemical Biology. The authors kindly thank Professor Michael Kertesz for providing the PARS gene. S.R.H. acknowledges predoctoral support from the ARCS foundation. L.J.W. thank the Skaggs Institute of Chemical Biology for a postdoctoral fellowship.

References and notes

1. Hanson, S. R.; Best, M. D.; Wong, C. H. *Angew. Chem., Int. Ed.* **2004**, *43*, 5736–5763.
2. Neufeld, E. F. M. J.; Muenzer, J. The Mucopolysaccharidoses, 8th ed.. In *The Metabolic and Molecular Bases of Inherited Disease*; Scriver, C. R., Beaudet, A. L., Sly, W. S., Valle, D., Eds.; McGraw-Hill: New York, 1999; Vol. III, pp 3421–3452.
3. Ballabio, A.; Shapiro, L. J. Steroid Sulfatase Deficiency and X-linked Ichthyosis, 8th ed.. In *The Metabolic and Molecular Bases of Inherited Disease*; Scriver, C. R., Beaudet, A. L., Sly, W. S., Valle, D., Eds.; McGraw-Hill: New York, 1999; Vol. III, pp 4241–4261.
4. von Figura, K.; Gieselmann, V.; Joeken, J. Metachromatic Leukodystrophy, 8th ed.. In *The Metabolic and Molecular Bases of Inherited Disease*; Scriver, C. R., Beaudet, A. L., Sly, W. S., Valle, D., Eds.; McGraw-Hill: New York, 1999; Vol. III, pp 3695–3724.
5. Hopwood, J. J.; Ballabio, A. Multiple Sulfatase Deficiency and the Nature of the Sulfatase Family, 8th ed.. In *The Metabolic and Molecular Bases of Inherited Disease*; Scriver, C. R., Beaudet, A. L., Sly, W. S., Valle, D., Eds.; McGraw-Hill: New York, 1999; Vol. III, pp 3725–3732.
6. Roberton, A. M.; Wright, D. P. *Can. J. Gastroenterol.* **1997**, *11*, 361–366.
7. Dhoot, G. K.; Gustafsson, M. K.; Ai, X.; Sun, W.; Standiford, D. M.; Emerson, C. P., Jr. *Science* **2001**, *293*, 1663–1666.
8. Schirmer, A.; Kolter, R. *Chem. Biol.* **1998**, *5*, R181–R186.
9. Uhlhorn-Dierks, G.; Kolter, T.; Sandhoff, K. *Angew. Chem., Int. Ed.* **1998**, *37*, 2453–2455.
10. Sardiello, M.; Annunziata, I.; Roma, G.; Ballabio, A. *Hum. Mol. Genet.* **2005**, *14*, 3203–3217.
11. Lukatela, G.; Krauss, N.; Theis, K.; Selmer, T.; Gieselmann, V.; von Figura, K.; Saenger, W. *Biochemistry* **1998**, *37*, 3654–3664.
12. Parenti, G.; Meroni, G.; Ballabio, A. *Curr. Opin. Genet. Dev.* **1997**, *7*, 386–391.
13. Nussbaumer, P.; Billich, A. *Med. Res. Rev.* **2004**, *24*, 529–576.
14. Ai, X.; Do, A.-T.; Lozynska, O.; Kusche-Gullberg, M.; Lindahl, U.; Emerson, C. P., Jr. *J. Cell Biol.* **2003**, *162*, 341–351.
15. Lai, J.; Chien, J.; Staub, J.; Avula, R.; Greene, E. L.; Matthews, T. A.; Smith, D. I.; Kaufmann, S. H.; Roberts, L. R.; Shridhar, V. *J. Biol. Chem.* **2003**, *278*, 23107–23117.
16. Roberton, A. M.; Corfield, A. P. *Mucin Degradation and its Significance in Inflammatory Conditions of the GI Tract*; Kluwer Academic: Great Britain, 1999, pp 222–261.
17. Roberton, A. M.; Wiggins, R.; Horner, P. J.; Greenwood, R.; Crowley, T.; Fernandes, A.; Berry, M.; Corfield, A. P. *J. Clin. Microbiol.* **2005**, *43*, 5504–5508.
18. Winum, J. Y.; Scozzafava, A.; Montero, J. L.; Supuran, C. T. *Med. Res. Rev.* **2005**, *25*, 186–228.
19. Abeles, R. H.; Maycock, A. L. *Accounts of Chemical Research.* **1976**, *9*, 313–319.
20. Beil, S.; Kehrli, H.; James, P.; Staudenmann, W.; Cook, A. M.; Leisinger, T.; Kertesz, M. A. *Eur. J. Biochem.* **1995**, *229*, 385–394.
21. Boltes, I.; Czapinska, H.; Kahnert, A.; von Bulow, R.; Dierks, T.; Schmidt, B.; vonFigura, K.; Kertesz, M. A.; Uson, I. *Structure* **2001**, *9*, 483–491.
22. Speers, A. E.; Cravatt, B. F. *Chem. Biol.* **2004**, *11*, 535–546.
23. Cesaro-Tadic, S.; Lagos, D.; Honegger, A.; Rickard, J. H.; Partridge, L. J.; Blackburn, G. M.; Pluckthun, A. *Nat. Biotechnol.* **2003**, *21*, 679–685.
24. O'Brien, P. J.; Herschlag, D. *J. Am. Chem. Soc.* **1998**, *120*, 12369–12370.
25. Liu, Y.; Lien, I. F. F.; Ruttgaizer, S.; Dove, P.; Taylor, S. D. *Org. Lett.* **2004**, *6*, 209–212.
26. von Bulow, R.; Schmidt, B.; Dierks, T.; von Figura, K.; Uson, I. *J. Mol. Biol.* **2001**, *305*, 269–277.
27. Howarth, N. M.; Purohit, A.; Reed, M. J.; Potter, B. V. L. *J. Med. Chem.* **1994**, *37*, 219–221.
28. Hernandez-Guzman, F. G.; Higashiyama, T.; Pangborn, W.; Osawa, Y.; Ghosh, D. *J. Biol. Chem.* **2003**, *278*, 22989–22997.
29. Purohit, A.; Williams, G. J.; Howarth, N. M.; Potter, B. V. L.; Reed, M. J. *Biochemistry* **1995**, *34*, 11508–11514.
30. Woo, L. W. L.; Purohit, A.; Malini, B.; Reed, M. J.; Potter, B. V. L. *Chem. Biol.* **2000**, *7*, 773–791.
31. Ahmed, S.; James, K.; Owen, C. P.; Patel, C. K.; Sampson, L. *Bioorg. Med. Chem. Lett.* **2002**, *12*, 1279–1282.
32. Peters, R. H.; Chao, W.-R.; Sato, B.; Shigeno, K.; Zaveri, N. T.; Tanabe, M. *Steroids* **2003**, *68*, 97–110.
33. Kitz, R.; Wilson, I. B. *J. Biol. Chem.* **1962**, *237*, 3245–3249.

34. Woo, L. W. L.; Purohit, A.; Reed, M. J.; Potter, B. V. L. *Bioorg. Med. Chem. Lett.* **1997**, *7*, 3075–3080.
35. Bond, C. S.; Clements, P. R.; Ashby, S. J.; Collyer, C. A.; Harrop, S. J.; Hopwood, J. J.; Guss, J. M. *Structure* **1997**, *5*, 277–289.
36. Jessani, N.; Cravatt, B. F. *Curr. Opin. Chem. Biol.* **2004**, *8*, 54–59.
37. Chapman, E.; Bryan, M. C.; Wong, C.-H. *Proc. Natl. Acad. Sci. U.S.A.* **2003**, *100*, 910–915.
38. Andersen, K. K.; Bray, D. D.; Chumpradit, S.; Clark, M. E.; Habgood, G. J.; Hubbard, C. D.; Young, K. M. *J. Org. Chem.* **1991**, *56*, 6508–6516.
39. Andersen, K. K.; Kociolek, M. G. *J. Org. Chem.* **1995**, *60*, 2003–2007.